



Article

Binary Promoter Improving the Moderate-Temperature Adhesion of Addition-Cured Liquid Silicone Rubber for Thermally Conductive Potting

Jia-Kai Wu ^{1,2}, Kai-Wen Zheng ¹ , Qiong-Yan Wang ^{2,*}, Xin-Cheng Nie ², Rui Wang ² and Jun-Ting Xu ¹ 

- ¹ MOE Key Laboratory of Macromolecular Synthesis and Functionalization, Department of Polymer Science & Engineering, Zhejiang University, Hangzhou 310027, China; 11429008@zju.edu.cn (J.-K.W.); 15117965820@163.com (K.-W.Z.); xujt@zju.edu.cn (J.-T.X.)
- ² Research and Development Center, Zhejiang Sucon Silicone Co., Ltd., Shaoxing 312088, China; sxyxnc@163.com (X.-C.N.); wangrhyc88@163.com (R.W.)
- * Correspondence: wqy2040@163.com

Abstract: The strong adhesion of thermally conductive silicone encapsulants on highly integrated electronic devices can avoid external damages and lead to an improved long-term reliability, which is critical for their commercial application. However, due to their low surface energy and chemical reactivity, the self-adhesive ability of silicone encapsulants to substrates need to be explored further. Here, we developed epoxy and alkoxy groups-bifunctionalized tetramethylcyclotetrasiloxane (D₄H-MSEP) and boron-modified polydimethylsiloxane (PDMS-B), which were synthesized and utilized as synergistic adhesion promoters to provide two-component addition-cured liquid silicone rubber (LSR) with a good self-adhesion ability for applications in electronic packaging at moderate temperatures. The chemical structures of D₄H-MSEP and PDMS-B were characterized by Fourier transform infrared spectroscopy. The mass percentage of PDMS-B to D₄H-MSEP, the adhesion promoters content and the curing temperature on the adhesion strength of LSR towards substrates were systematically investigated. In detail, the LSR with 2.0 wt% D₄H-MSEP and 0.6 wt% PDMS-B exhibited a lap-shear strength of 1.12 MPa towards Al plates when curing at 80 °C, and the cohesive failure was also observed. The LSR presented a thermal conductivity of 1.59 W m⁻¹ K⁻¹ and good fluidity, which provided a sufficient heat dissipation ability and fluidity for potting applications with 85.7 wt% loading of spherical α-Al₂O₃. Importantly, 85 °C and 85% relative humidity durability testing demonstrated LSR with a good encapsulation capacity in long-term processes. This strategy endows LSR with a good self-adhesive ability at moderate temperatures, making it a promising material requiring long-term reliability in the encapsulation of temperature-sensitive electronic devices.

Keywords: binary promoter; liquid silicone rubber; thermally conductive; moderate-temperature adhesion



Citation: Wu, J.-K.; Zheng, K.-W.; Wang, Q.-Y.; Nie, X.-C.; Wang, R.; Xu, J.-T. Binary Promoter Improving the Moderate-Temperature Adhesion of Addition-Cured Liquid Silicone Rubber for Thermally Conductive Potting. *Materials* **2022**, *15*, 5211. <https://doi.org/10.3390/ma15155211>

Academic Editor: Klaus Werner Stöckelhuber

Received: 8 June 2022

Accepted: 21 July 2022

Published: 28 July 2022

Publisher's Note: MDPI stays neutral with regard to jurisdictional claims in published maps and institutional affiliations.



Copyright: © 2022 by the authors. Licensee MDPI, Basel, Switzerland. This article is an open access article distributed under the terms and conditions of the Creative Commons Attribution (CC BY) license (<https://creativecommons.org/licenses/by/4.0/>).

1. Introduction

Optical, electronic devices and electrical modules are continuously evolving in functionality and achieving high performance while tending to be smaller and more integrated [1–4]. These devices are generally encapsulated with polymeric potting materials to achieve heat transfer and avoid environmental damages (e.g., moisture penetration and mechanical damage), thus boosting their long-term reliability [5–7]. Addition-cured liquid silicone rubber (LSR) possesses an amazing array of properties including a high dielectric breakdown strength, flame resistance, heat and cold resistance, stress relieving properties and long-lasting durability, which make it one of the most promising materials for the protection of electronic devices [8,9]. The poor mechanical properties of pure LSR limit its practical applications [9]. Researchers have expended great efforts to incorporate reinforcement fillers and functional fillers into LSR to improve its mechanical properties

and introduce additional properties such as thermal conductivity and electrical conductivity [10–13]. LSR can be imparted with suitable thermal conductivity for efficient heat dissipation by doping with high thermal conductivity fillers such as carbon-based fillers, boron nitride, aluminum nitride, aluminum oxide (Al_2O_3) and so on [12–16].

Hydrophobic spherical α - Al_2O_3 -contained LSR (LSR/ Al_2O_3) achieves a high thermal conductivity ($>1.0 \text{ W m}^{-1} \text{ K}^{-1}$) and high fluidity while maintaining a low viscosity ($<10,000 \text{ mPa}\cdot\text{s}$), which are key properties for workability during the encapsulation [16–18]. Thus, LSR/ Al_2O_3 composites have been widely used in the application of electronic devices encapsulation. However, addition-cured LSR presents a low surface energy and chemical reactivity, leading to a weak adhesion ability towards substrates [19,20]. Such weakly bonded interface is vulnerable to moisture erosion or damage from external forces, which can deteriorate the encapsulation effect of LSR in electronic devices operating in harsh environments [21–24]. Considerable efforts have been made to enhance the adhesion ability of LSR towards substrates, including primer pretreatment, substrate surface modification, the addition of an adhesion promoter, etc. [25–29]. Primers consisting of highly reactive molecules and solvents exhibit film-forming properties, good chemical reactivity and excellent wettability to most substrates, which are beneficial to enhancing the interfacial adhesion ability of LSR [25]. Grard et al. utilized xylene-diluted silane coupling agent mixtures as a primer to treat an AA6061 aluminum alloy surface to enhance its adhesion strength to silicone rubber [26]. The silicone rubber/aluminum alloy assembly showed a peel strength of 6.7 N m^{-1} and a 100% cohesive failure during a 90° -peel test. The substrate surface modification is an effective method to improve the adhesion strength of LSR to other materials by generating new reactive groups on the substrate surface. Roth et al. performed oxygen and ammonia plasma treatments on silicone rubber and the subsequent grafting of poly(ethylene-alt-maleic anhydride) to form a functionalized surface [27]. The modified silicone rubber showed improved permanent adhesion with epoxy resin and yielded a pull-off strength of 4.7 MPa. The above-mentioned methods can effectively improve the adhesion of LSR to various substrates; however, both methods are time-consuming and complicated processes, and they are harmful to the environment. Therefore, the addition of adhesion promoters into LSR to provide a self-adhesive capacity has spurred intensive research interest due to the simple and scalable process and eco-friendly properties [29–33]. Pan et al. reported a vinyl and epoxy groups-functionalized silane oligomer and used it as an adhesion promoter to prepare a self-adhesive addition-cure silicone encapsulant [32]. The LSR/ Al_2O_3 encapsulant showed a shear strength of 1.06 MPa towards the Al substrate with a 2 wt% addition of an adhesion promoter after curing at 130°C , which was about 2.12 times higher than that of LSR without adding an adhesion promoter. Epoxy, alkoxy and acrylate groups-modified prepolymer was synthesized by Wang et al. and was utilized as an adhesion promoter to improve the adhesion strength between LSR and the Al substrate [34]. The adhesion strength was effectively improved by 161% by incorporating 10.0 wt% of the prepared adhesion promoter in LSR. These reactive groups (i.e., epoxy, alkoxy and methacryloxy groups)-containing adhesion promoters generally demonstrated their great improvement in bonding performance at high working temperatures ($>120^\circ\text{C}$). However, most of the adhesion promoters are unable to offer an efficient adhesion ability for LSR at moderate curing temperatures (e.g., 80°C) [31–33]. Therefore, it remains a challenge to achieve efficient encapsulation and provide long-term reliable protection for temperature-sensitive electronic devices.

The inefficiency of adhesion promoters is mainly derived from the low reactivity of epoxy groups at moderate temperatures [35]. In this work, an additional co-adhesive is designed to increase the reactivity of epoxy groups and to impart a good self-adhesion ability for applications in electronic packaging at moderate temperature. To this end, allyl dioxaborane-modified polydimethylsiloxane (PDMS-B) was synthesized and served as a co-adhesive to collaborate with olefin-based epoxy and alkoxy groups-bifunctionalized tetramethylcyclotetrasiloxane ($\text{D}_4\text{H-MSEP}$) so as to offer the two-component addition-cured LSR with a good self-adhesion ability at moderate temperatures. The olefin-containing

reactive groups and siloxane backbones endowed the adhesion promoters with a good compatibility with LSR, while the boron-containing groups were designed to facilitate the curing of epoxy groups. By incorporating two components, PDMS-B and D₄H-MSEP, into LSR together, the as-prepared two-component addition-curing LSR presented good stability during storage and exhibited high reactivity and adhesion. The effect of the weight percentage of PDMS-B to D₄H-MSEP and the content of adhesion promoters on the adhesion strength of LSR were systematically investigated. Additionally, the durability test at a temperature of 85 °C and a relative humidity of 85% was performed to evaluate the long-term stability of LSR and its encapsulation capacity.

2. Materials and Methods

2.1. Materials

Allyltrimethoxysilane (ATMS, >97.0%), 1,2-epoxy-5-hexene (EPHE, >96.0%), 2-allyl-4,4,5,5-tetramethyl-1,3,2-dioxaborolane (ATDB, ≥95%), 2,4,6,8-tetramethylcyclotetrasiloxane (D₄H, 98%) and 3-methyl-1-pentyn-3-ol (98%), toluene (GR) were all purchased from Macklin Inc. Shanghai, China (www.macklin.cn, accessed on 1 February 2022). Vinyl-terminated polydimethylsiloxane with a reduced volatility (PDMS-Vi, viscosity of ~230 mPa·s, product code: HYC-Vi230E) and hydride-terminated poly(methylhydro-co-dimethylsiloxane) (PHMS-H, viscosity of ~10 mPa·s, product Code: HYC-LH-0.5) were obtained from Zhejiang Sucon Silicone Co., Ltd., Shaoxing, China (www.hycsilicon.com, accessed on 1 June 2022). Monovinyl-terminated polydimethylsiloxane (PDMS-mVi, asymmetric, 500 mPa·s, product code: MCR-V25) was obtained from Gelest, Inc., Morrisville, PA, USA (www.gelest.com, accessed on 1 November 2021). Spherical α -Al₂O₃ modified by a silane coupling agent (BAH series) was acquired from Shanghai Bestry Performance Materials Co., Ltd., Shanghai, China (www.bestry-tech.com, accessed on 1 November 2021). The Karstedt's platinum catalyst with a platinum content of 5000 ppm was obtained from Heraeus Materials Technology Shanghai Ltd., Shanghai, China (www.heraeus.cn, accessed on 1 June 2021).

2.2. Synthesis of Boron-Modified PDMS

Boron-modified PDMS (PDMS-B) was synthesized through a hydrosilylation reaction between ATDB and PHMS-H, as shown in Figure 1 Route A. The detailed synthesis procedure was as follows: PHMS-H (10.0 g) was dissolved in anhydrous toluene (20.0 mL) in a four-neck round bottom flask equipped with a temperature sensor, a dropping funnel, a reflux condenser and nitrogen-blow devices. The reaction solution was kept at 20 °C for 30 min to reach the pre-equilibration, followed by adding Karstedt's platinum catalyst (0.02 g) into the solution. Subsequently, excessive ATDB (10.0 g) was added dropwise into the flask through the dropping funnel in 10 min, the reaction mixture was stirred for 2 h and then temperature was increased to 60 °C until all Si-H groups were reacted. The unreacted ATDB and toluene were removed through a thin-film evaporator at 60 °C and 200 Pa to yield the desired product PDMS-B as a colorless, transparent and viscous liquid.

2.3. Synthesis of Epoxy and Alkoxy Groups-Bifunctionalized D₄H

The synthetic pathway of epoxy and alkoxy groups-bifunctionalized D₄H is illustrated below (Figure 1 Route B): typically, ATMS (6.48 g, 40.0 mmol) and EPHE (3.92 g, 40.0 mmol) were dissolved in anhydrous toluene (20.0 mL) in the aforementioned four-neck round bottom flask. After adding Karstedt's platinum catalyst (0.01 g), the flask was pre-equilibrated with N₂ for 30 min at 20 °C. D₄H (9.6 g, 40 mmol) was added dropwise into the solution for 10 min under vigorous stirring. After all of the -CH = CH₂ groups from ATMS and EPHE were reacted, which was monitored by Fourier-transform infrared spectroscopy (stretching vibration of -CH = CH₂ groups: 1640 cm⁻¹), the solution was mixed with activated carbon for 2 h and filtrated through a 0.22 μ m filter to remove the residual platinum catalyst. The unreacted monomers and toluene were removed through the thin-film evaporator to yield the epoxy and alkoxy bifunctional D₄H-MSEP as a colorless and transparent liquid.

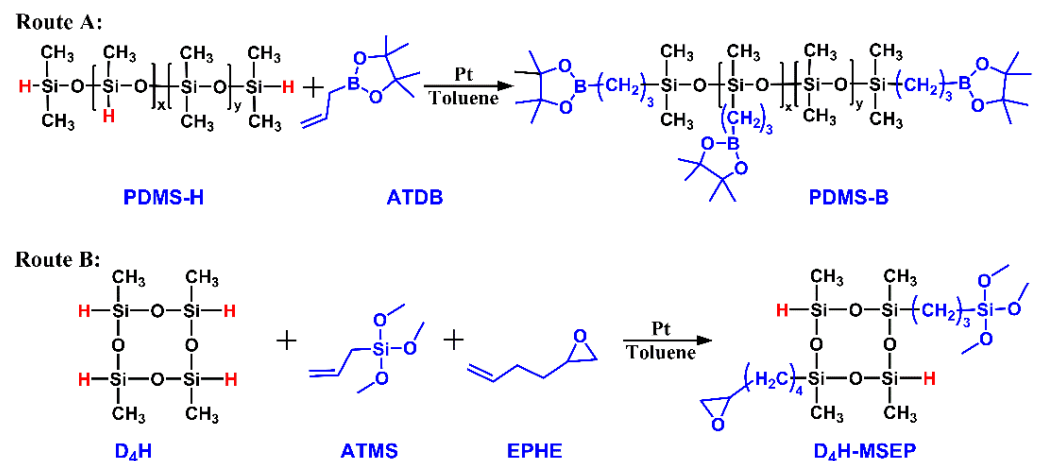


Figure 1. Schematic diagram for the synthesis of (A) PDMS-B and (B) D₄H-MSEP.

2.4. Preparation of Self-Adhesive Two-Component Addition-Curing LSR

PDMS-Vi, PDMS-mVi and Al₂O₃ were kneaded with a planetary mixer for 30 min in the designed amounts, as shown in Table 1, followed by a heat treatment at 150 °C and a vacuum of 500 Pa for 1 h to promote the uniform dispersion of Al₂O₃ in the PDMS matrix. Subsequently, the Karstedt's platinum catalyst and PDMS-B were added in the cooled PDMS/Al₂O₃ matrix and kneaded for 30 min under vacuum conditions to obtain the component A of the two-component LSR. PDMS-Vi, PDMS-mVi and Al₂O₃ were treated as above to obtain uniform liquid silicone rubber blends. PHMS-H, D₄H-MSEP and 3-methyl-1-pentyn-3-ol (platinum inhibitor) were mixed with a cooled PDMS/Al₂O₃ matrix under vacuum conditions to obtain the silicone composite termed as the component B of the two-component LSR. Component A and component B were thoroughly stirred and then mixed in equal proportions to afford the two-component LSR. The LSR was deaired at a vacuum of 500 Pa for 2 min before using.

Table 1. Compositions of the two-component LSR.

Compositions	Content (g)	
	Component A	Component B
PDMS-Vi	75.0	66.0
PDMS-mVi	25.0	22.0
PHMS-H	/	12.0
Spherical α-Al ₂ O ₃ ¹	300–700	300–700
PDMS-B	0–9.6	/
D ₄ H-MSEP	/	0–32.0
Platinum catalyst	0.8	/
3-methyl-1-pentyn-3-ol	/	1.0

¹ The mass percentage of Al₂O₃ and silicone fluid is 300/100 to 700/100 in both component A and component B, equivalent to the Al₂O₃ contents of 75.0 to 87.5 wt% in LSR.

2.5. Characterization

2.5.1. Fourier Transform Infrared (FTIR) Analysis

FTIR measurements were performed on a ThermoFisher Scientific Nicolet iS10 spectrometer (USA) to identify the chemical structures of the synthesized PDMS-B and D₄H-MSEP. Samples (0.2 mL) were coated on KBr slices (25 mm × 2 mm) to form thin films for FTIR measurements.

2.5.2. Viscosity Measurement

The viscosity of PDMS/Al₂O₃ composites was measured using a Brookfield DV2T viscometer at 25 °C according to the ASTM D-445 standard. Three specimens were measured for each measurement, and the mean value was calculated.

2.5.3. Mechanical Properties Test

The tensile strength and elongation at break of the cured LSR samples were measured by a Gotech AI-7000S universal testing machine at a stretching rate of 50 mm min⁻¹ at 25 °C according to the GB/T 528 standard. Under 3000 MPa pressure, LSR samples were cured at 80 °C for 2 h and then at 25 °C for another 24 h to form a 2 mm-thick rectangular sheet. The samples were tailored into dumbbell shapes before mechanical tests. Five specimens were measured for each measurement, and the mean value was calculated.

2.5.4. Thermal Conductivities Test

The thermal conductivities of the LSR sheets (25 mm × 25 mm, 2 mm-thick) were tested by a thermal analyzer (TC3000E, Xiotech, Xi'an, China) according to the ASTM D-5930 standard. Five specimens were measured for each measurement, and the mean value was calculated.

2.5.5. Adhesion Performance

Tensile lap-shear strength tests were performed using a Gotech AI-7000S universal testing machine to evaluate the adhesion performance of the LSR towards Al and printed circuit board (PCB) plates (Figure 2), both of which are the major substrate materials for electronic devices. The Al and PCB plates were rinsed with isopropanol in an ultrasonic bath for 10 min at room temperature and then dried at 60 °C. Two-component LSR was potted into the tailored gap between two adherends and cured at 80 °C without any pressure followed by 25 °C for 24 h. The effective bonding surface of the LSR and adherends was 25 × 25 mm², and the thickness of the LSR was 2 mm. The lap-shear strength between the LSR and adherends was calculated as the following equation:

$$\tau_s = F_m / w \quad (1)$$

where τ_s , F_m and w are the lap-shear strength, maximum force and effective bonding surface, respectively. Five specimens were measured for each measurement, and the mean value was calculated.

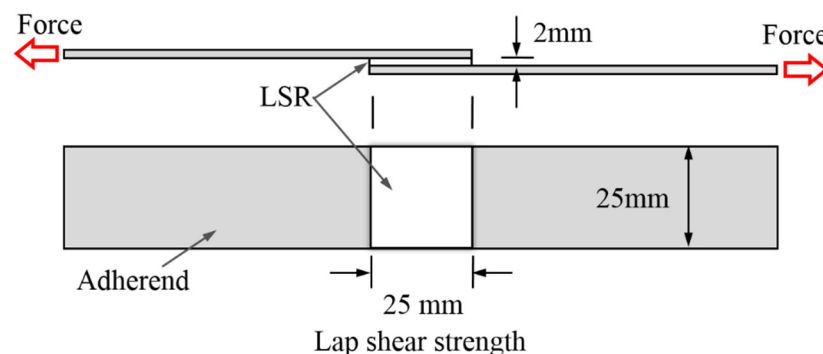


Figure 2. Schematic diagram of the tensile lap-shear strength test between the LSR and adherends.

3. Results

3.1. Structural Characterization of PDMS-B and D₄H-MSEP

The chemical structures of the raw materials and resultant PDMS-B and D₄H-MSEP were identified by FT-IR, as shown in Figure 3. In Figure 3a, the characteristic band of 1300–1500 cm⁻¹, with the peak centered at 1370 cm⁻¹ and the sharp peak at 1640 cm⁻¹, corresponded to the stretching vibration of B-O bonds and -CH = CH₂ groups in ATDB,

respectively [36–38]. The band in the range of 2080–2200 cm^{-1} was ascribed to the stretching vibration of -Si-H groups in PHMS-H. In the FT-IR spectrum of PDMS-B, the appearance of a new absorption peak for B-O bonds and the absence of an absorption peak for the -Si-H groups and $-\text{CH}=\text{CH}_2$ groups indicated the complete hydrosilylation reaction between PHMS-H and ATDB and the successful synthesis of boron-modified PDMS. In Figure 3b, the sharp absorption peak at 2170 cm^{-1} was assigned to -Si-H groups in D_4H . The characteristic absorption peaks at 2840 cm^{-1} and 910 cm^{-1} were ascribed to the stretching vibration of -Si-OCH₃ groups in the ATMS and epoxy groups in EPHE, respectively [39–41]. The appearance of new absorption peaks for -Si-OCH₃ groups and epoxy groups, the reduced absorption intensity of the peak for -Si-H groups and the disappearance of the absorption peak for $-\text{CH}=\text{CH}_2$ groups in the yielded D_4H -MSEP demonstrated that the epoxy groups and alkoxy groups-bifunctionalized D_4H was synthesized. Notably, partial Si-H groups were intentionally retained, as observed in the spectrum of D_4H -MSEP, in order to bind to the LSR matrix through hydrosilylation during the further curing process.

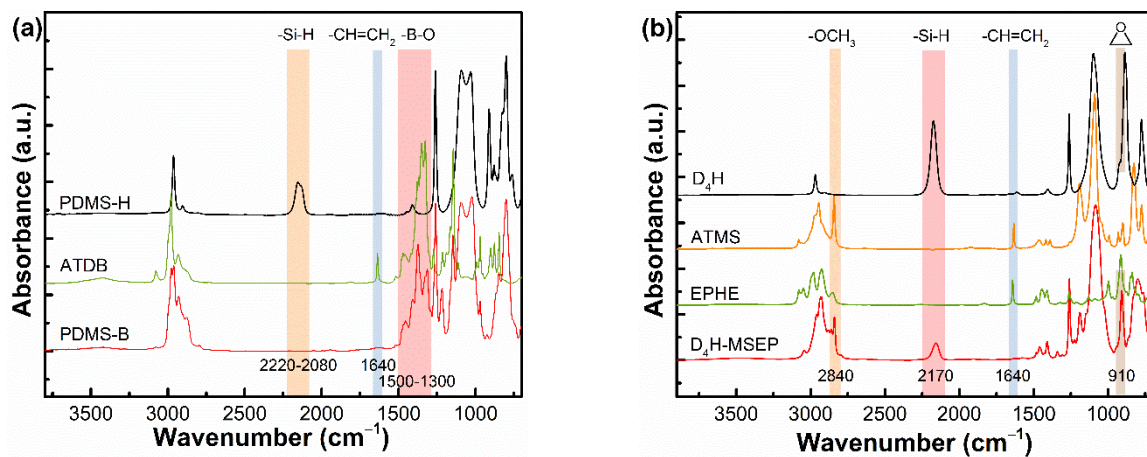


Figure 3. FT-IR spectra of (a) PDMS-H, ATDB and PDMS-B and (b) D_4H , ATMS, EPHE and D_4H -MSEP.

3.2. Thermal Conductivity and Mechanical Properties of LSR

The Al_2O_3 loading amount plays a key role in the thermal conductivity and viscosity of LSR, which directly affects the heat dissipation ability and potting processability. As shown in Figure 4, the thermal conductivity and viscosity of LSR monotonically increased with the increase in the Al_2O_3 content, and such an increasing trend is more obvious at a higher Al_2O_3 loading amount. In detail, the thermal conductivity of LSR increased from 0.78 $\text{W m}^{-1} \text{K}^{-1}$ to 1.81 $\text{W m}^{-1} \text{K}^{-1}$ as the Al_2O_3 content increased from 75 wt% to 87.5 wt%. The viscosity of LSR increased from 2622 mPa·s to 9185 mPa·s as the Al_2O_3 content increased from 75 wt% to 85.7 wt%. However, the viscosity increased dramatically to 14,452 mPa·s when the Al_2O_3 content increased to 87.5 wt%. The aggregation of Al_2O_3 and the intermolecular interaction between the Al_2O_3 agglomerates resulted in the rapidly increased viscosity of LSR, which made it unsuitable for potting applications in some complex devices where the viscosity should be less than 10,000 mPa·s. Therefore, the LSR with an 85.7 wt% Al_2O_3 loading amount, showing a thermal conductivity of 1.59 $\text{W m}^{-1} \text{K}^{-1}$ and a viscosity of 9185 mPa·s, was selected for the further improvement of the adhesion performance.

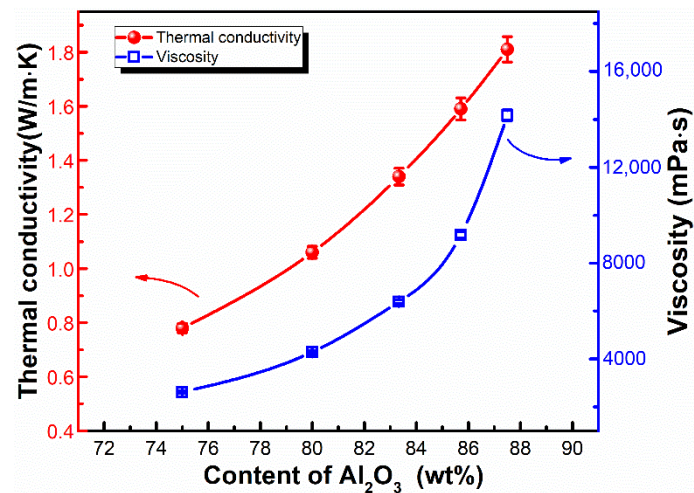


Figure 4. Dependences of the thermal conductivity and viscosity on the Al₂O₃ content in the LSR.

The effect of the Al₂O₃ content on the mechanical properties of the LSR were investigated and are shown in Figure 5. It was observed that the tensile strength and the elongation at break of the LSR were improved by the incorporation of the semi-reinforcing filler Al₂O₃. The optimal tensile strength of LSR reached up to 1.37 MPa with 83.3 wt% Al₂O₃ content, while the highest elongation at break reached up to 144.7% with 80.0 wt% Al₂O₃ content. However, the excessive incorporation of Al₂O₃ led to their aggregation, and the Al₂O₃ agglomerates act as defects in the LSR, reducing the effective interaction area between the particle and the matrix and hence the deterioration of the LSR mechanical properties. The LSR loaded with 85.7 wt% Al₂O₃ content, showing a tensile strength of 1.31 MPa and an elongation at break of 114%, was selected for the following studies.

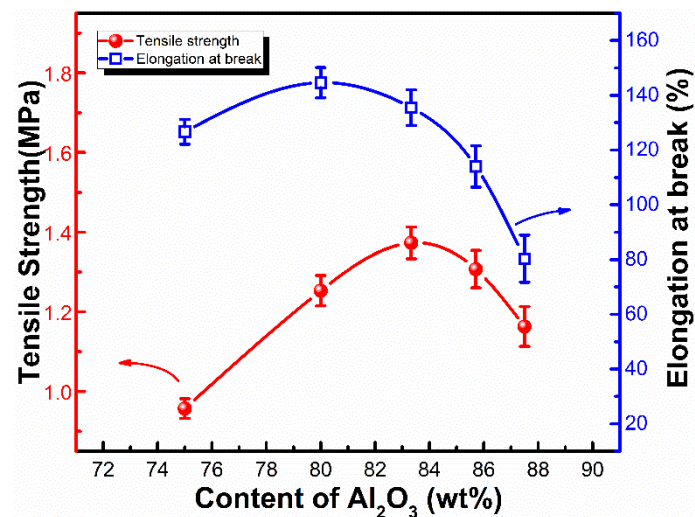


Figure 5. The mechanical properties of LSR with varied Al₂O₃ contents.

3.3. Adhesion Performance of LSR

Figure 6 presented the effect of PDMS-B and D₄H-MSEP content on the adhesion performance of LSR towards Al and PCB plates. The LSR containing 2.0 wt% D₄H-MSEP showed a weak bond strength towards both Al and PCB substrates after curing at 80 °C, which could be almost removed from the substrates (Figure 6b). Upon the addition of PDMS-B, however, both the LSR/Al and LSR/PCB joints (D₄H-MSEP content maintained at 2.0 wt%) showed remarkable enhancement in the lap-shear strength as the mass percentage of PDMS-B to D₄H-MSEP increased from 0 to 40%. In detail, the LSR/Al joints showed a lap-shear strength of 1.16 MPa as the mass percentage of PDMS-B to D₄H-MSEP approached

40%, which was 2.74 times higher than that of the LSR/Al joints (0.31 MPa) without adding PDMS-B. Moreover, the cohesive failure on the macroscale occurred at the interface of the LSR/Al joints when the mass percentage of PDMS-B to D₄H-MSEP reached up to 30% (Figure 6b). Further increasing the mass percentage of PDMS-B only led to a slight improvement in the lap-shear strength of the LSR/Al joints. Thus, the 30% mass percentage of PDMS-B to D₄H-MSEP can provide LSR with a sufficient adhesion ability. A similar enhancing trend of adhesion strength was also observed in LSR/PCB systems with increases in the PDMS-B content in LSR. These results demonstrated that the addition of PDMS-B indeed improved the adhesion ability of D₄H-MSEP-modified LSR. The boron atoms in PDMS-B promoted the reaction between epoxy groups and hydroxyl groups on the substrates [42]. The hydrolysis of the dioxaborolane groups into boron hydroxyl groups during the curing process facilitated the strong interactions between the polar groups from the substrates and the alkoxy groups from the D₄H-MSEP. By incorporating PDMS-B (in component A) and D₄H-MSEP (in component B) into two components, the as-prepared addition-curing LSR presented good stability during storage and exhibited high reactivity and adhesion during the curing process.

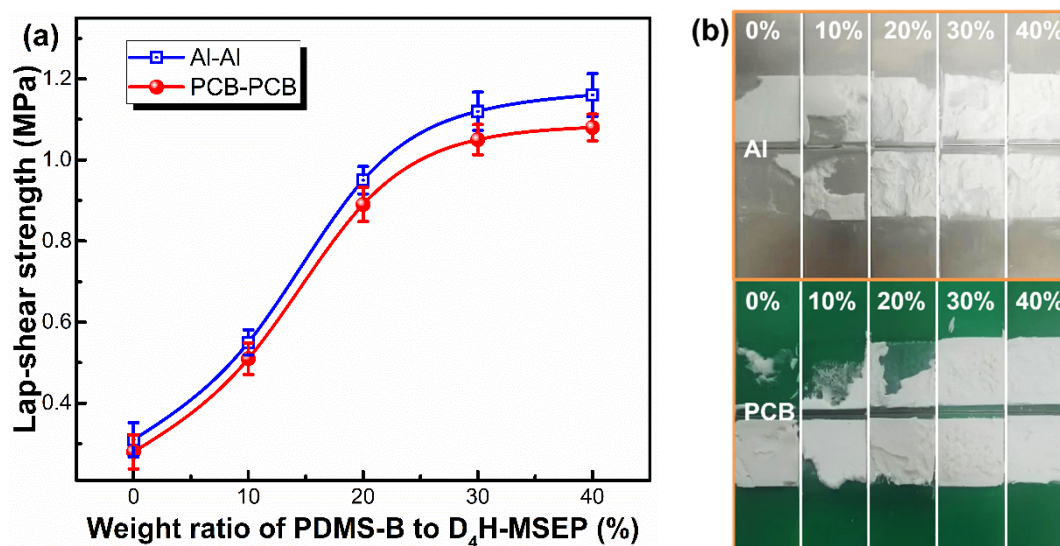


Figure 6. (a) Effect of the mass percentage of PDMS-B to D₄H-MSEP on the lap-shear strength of LSR/Al and LSR/PCB joints, (b) optical photographs of LSR/Al and LSR PCB joints after lap-shear strength tests. The mass percentage of PDMS-B to D₄H-MSEP was 0, 10, 20, 30 and 40%, respectively (LSR with 85.7 wt% Al₂O₃ and 2.0 wt% D₄H-MSEP; curing temperature: 80 °C).

The effect of D₄H-MSEP content on the lap-shear strength of LSR and adherends joints was investigated and is shown in Figure 7. Without the addition of an adhesion promoter, the LSR showed almost no adhesion to adherends due to its low surface energy and low surface activity, leading to the easy removal of LSR from the adherend surfaces. In contrast, the lap-shear strength between the LSR and Al (PCB) plates significantly increased to 1.04 MPa as the D₄H-MSEP content increased to 1.5 wt% (mass percentage of PDMS-B to D₄H-MSEP was kept at 30%), followed by a smooth enhancement approaching 1.12 MPa with the further increase in D₄H-MSEP content to 2.0 wt%. Increasing the adhesion promoter content would facilitate the enrichment of PDMS-B and D₄H-MSEP molecules on the LSR surface, hence improving the adhesion strength of LSR. The concentration of the adhesion promoter molecules at the interface was limited owing to the steric hindrance; however, the lap-shear strength showed a limited enhancement when the adhesion promoters content exceeded 1.5 wt%. Overall, these results confirmed that the high reactivity and interface enrichment of the binary adhesion promoters PDMS-B and D₄H-MSEP provided a synergistic effect on the enhancement of LSR adhesion performance and endowed the LSR with a great adhesion ability at a moderate temperature of 80 °C.

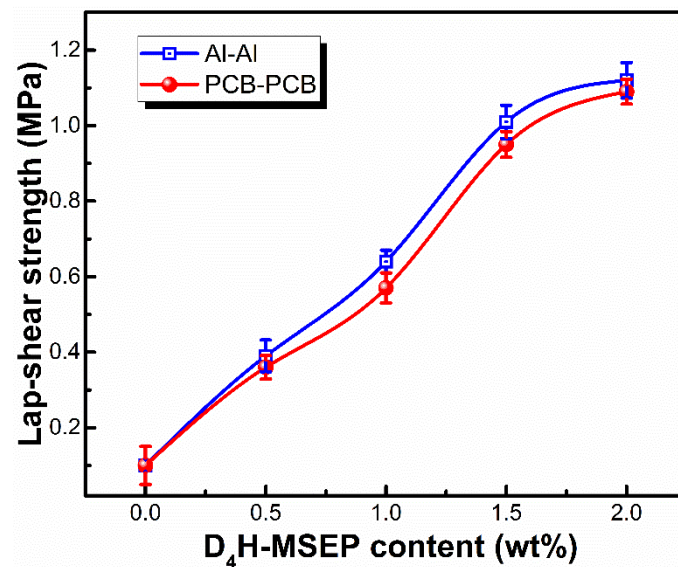


Figure 7. Effect of D₄H-MSEP content in LSR on the lap-shear strength of LSR/Al and LSR/PCB joints (LSR with 85.7 wt% Al₂O₃; curing temperature: 80 °C; PDMS-B/D₄H-MSEP = 30.0 wt%).

Figure 8 presents the effect of the curing temperature on the adhesion strength of LSR with adherends. The LSR exhibited a gradually enhanced lap-shear strength towards both Al and PCB plates as the curing temperature increased from 60 to 90 °C, resulting from the faster diffusion of the adhesion promoters to the LSR surface and the higher reactivity of the epoxy groups in D₄H-MSEP at higher curing temperatures. When the curing temperature reached 80 °C, the lap-shear strength of the LSR towards both of the two adherends was higher than 1.0 MPa, and the cohesive failure was observed at the interface of the LSR/adherends joints after lap-shear strength testing. This result indicated that the obtained LSR could be used for the encapsulation of temperature-sensitive materials such as plastic seals and sensitive electronic components. The LSR encapsulant prepared in this work is compared against the addition-cured silicone encapsulants reported in the literature and commercial products (Table 2). The LSR potting compound described in this paper can achieve effective adhesion at lower temperatures.

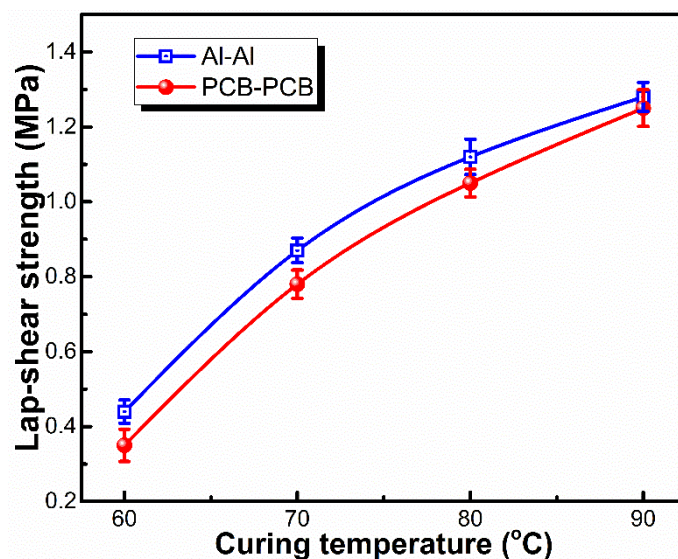


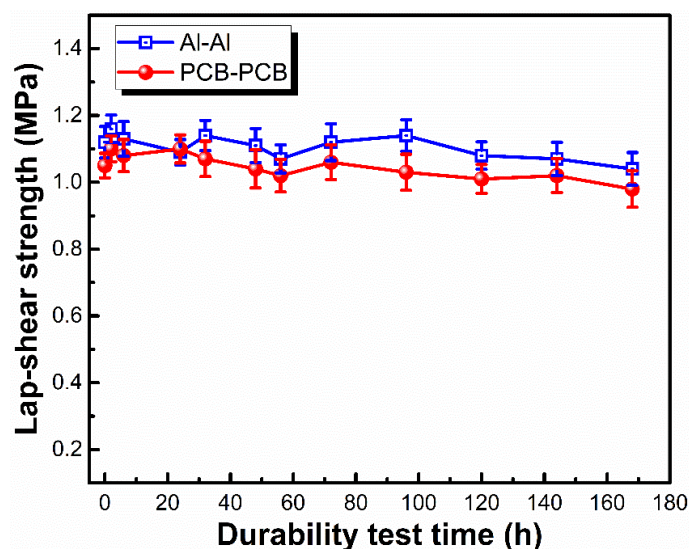
Figure 8. Effect of curing temperature on the lap-shear strength of LSR/Al and LSR/PCB joints (LSR with 85.7 wt% Al₂O₃, 0.6 wt% PDMS-B and 2.0 wt% D₄H-MSEP; curing temperature: 80 °C).

Table 2. Performance comparison of the LSR prepared in this work with the addition-cured LSR encapsulants reported in the literature and commercial products.

Adhesion Promoter	Substrates	Curing Temperature	Shear Strength	Ref.
Siloxane oligomers-containing boron and epoxy groups	Cu/Cu	150 °C	3.16 MPa	[30]
Vinyl and epoxy groups-modified silane oligomer	Al/Al	130 °C	1.06 MPa	[32]
Phenyl silicone resin with epoxy and acrylate groups	Al/Al	150 °C	4.43 MPa	[33]
Epoxy, alkoxy and acrylate groups-modified prepolymer	Al/Al	100 °C	0.83 MPa	[34]
KE-1285-A/B ¹	Al/Al	120 °C	1.50 MPa	[18]
Dow Corning [®] SE 1816 CV Kit ²	Al/Al	150 °C	1.80 MPa	[43]
D ₄ H-MSEP/PDMS-B	Al/Al	80 °C	1.12 MPa	This work

¹ Commercial silicone encapsulant of Shin-Etsu Silicone, Japan. ² Commercial silicone encapsulant of Dow Corning, Midland, MI, USA.

The encapsulation with silicone potting materials can improve the device operation reliability and durability, which is critical for optical and electronic applications including fiber optic bundles, sensors, insulated gate bipolar transistors and so on [44]. The temperature of 85 °C and the relative humidity of 85% were set to carry out the durability testing so as to accelerate the evaluation of the device performance. The dependence of lap-shear strength on testing time was investigated to evaluate the long-term reliability of LSR for device encapsulation [45]. As shown in Figure 9, the lap-shear strength of LSR towards both Al and PCB plates was almost unchanged during the 200 h testing period. This good, durable adhesion would provide long-term protection for a variety of optical and electronic devices.

**Figure 9.** Lap-shear strength of LSR with the durability test time at 85 °C/85% RH condition (LSR with 85.7 wt% Al₂O₃, 0.6 wt% PDMS-B and 2.0 wt% D₄H-MSEP; curing temperature: 80 °C).

4. Conclusions

Binary adhesion promoters, boron-modified PDMS-B and epoxy and alkoxy groups-bifunctionalized D₄H-MSEP, were synthesized in order to provide an addition-cured thermally conductive LSR encapsulant with a strong self-adhesion ability at moderate temperatures. The thermal conductivity, viscosity and mechanical and adhesion properties of the LSR encapsulant were systematically investigated. In detail, the LSR containing 2.0 wt% D₄H-MSEP and 0.6 wt% PDMS-B showed a lap-shear strength of 1.12 MPa to-

wards the Al plate when curing at 80 °C. The cohesive failure occurred at the interfaces of both the LSR/Al and LSR/PCB joints. The LSR with an 85.7 wt% Al₂O₃ loading content provided a sufficient heat dissipation ability and fluidity for potting applications. Importantly, durability testing at the temperature of 85 °C and at 85% relative humidity suggested that LSR features a good encapsulation capacity during a long-term operation. This design strategy endows LSR with long-term reliability for further potential applications in the encapsulation of temperature-sensitive optical and electronic devices at specific working temperatures.

Author Contributions: Conceptualization, J.-K.W., J.-T.X. and Q.-Y.W.; methodology, J.-K.W., X.-C.N. and R.W.; formal analysis, K.-W.Z.; investigation, J.-K.W.; resources, Q.-Y.W.; data curation, J.-K.W.; writing—original draft preparation, J.-K.W.; writing—review and editing, J.-T.X. and K.-W.Z.; visualization, J.-K.W.; supervision, Q.-Y.W.; funding acquisition, Q.-Y.W. All authors have read and agreed to the published version of the manuscript.

Funding: This study has been funded by Zhejiang Sucon Silicone Co., Ltd. (Sucon2020051602Y).

Institutional Review Board Statement: Not applicable.

Informed Consent Statement: Not applicable.

Data Availability Statement: Not applicable.

Conflicts of Interest: The authors declare no conflict of interest.

References

1. Ziar, H.; Manganiello, P.; Isabella, O.; Zeman, M. Photovoltaics: Intelligent PV-based devices for energy and information applications. *Energ. Environ. Sci.* **2021**, *14*, 106–126. [[CrossRef](#)]
2. Watanabe, A.O.; Ali, M.; Sayeed, S.Y.B.; Tummala, R.R.; Pulugurtha, M.R. A review of 5G Front-End systems package integration. *IEEE Trans. Compon. Packag. Manuf. Technol.* **2021**, *11*, 118–133. [[CrossRef](#)]
3. Ramirez, J.M.; Malhouitre, S.; Gradkowski, K.; Morrissey, P.E.; O'Brien, P.; Caillaud, C.; Vaissiere, N.; Decobert, J.; Lei, S.; Enright, R.; et al. III-V-on-Silicon integration: From hybrid devices to heterogeneous photonic integrated circuits. *IEEE J. Sel. Top. Quant.* **2020**, *26*, 6100213. [[CrossRef](#)]
4. Chen, C.; Luo, F.; Kang, Y. A review of SiC power module packaging: Layout, material system and integration. *CPSS Trans. Power Electron. Appl.* **2017**, *2*, 170–186. [[CrossRef](#)]
5. Li, R.; Wang, Y.; Zhang, C.; Liang, H.; Li, J.; Du, B. Non-Linear conductivity Epoxy/SiC composites for emerging power module packaging: Fabrication, characterization and application. *Materials* **2020**, *13*, 3278. [[CrossRef](#)] [[PubMed](#)]
6. Zhao, Z.J.; Zhu, Z.X.; Zhang, H.; Wang, F.; Jiang, W.J.; Lin, S.; Yang, Y. Polyurethane sponge-derived nitrogen-doped carbon-encapsulation composite for enhanced lithium-ion battery performances. *Appl. Surf. Sci.* **2020**, *534*, 147631. [[CrossRef](#)]
7. Otsuka, K.; Shirai, Y.; Okutani, K. A new silicone gel sealing mechanism for high reliability encapsulation. *IEEE Trans. Comp. Hybrids Manuf. Technol.* **1984**, *3*, 249–256. [[CrossRef](#)]
8. Shit, S.C.; Shah, P. A Review on Silicone Rubber. *Natl. Acad. Sci. Lett.* **2013**, *36*, 355–365. [[CrossRef](#)]
9. Fink, J.K. *Liquid Silicone Rubber: Chemistry, Materials, and Processing*; John Wiley & Sons: Hoboken, NJ, USA, 2019.
10. Bahrain, S.H.K.; Masdek, N.R.N.; Mahmud, J.; Mohammed, M.N.; Sapuan, S.M.; Ilyas, R.A.; Mohamed, A.; Shamseldin, M.A.; Abdelrahman, A.; Asyraf, M.R.M. Morphological, physical, and mechanical properties of Sugar-Palm (*Arenga pinnata* (Wurmb) Merr.)-Reinforced silicone rubber biocomposites. *Materials* **2022**, *15*, 4062. [[CrossRef](#)]
11. Bahrain, S.H.K.; Rahim, N.N.C.A.; Mahmud, J.; Mohammed, M.N.; Sapuan, S.M.; Ilyas, R.A.; Alkhatib, S.E.; Asyraf, M.R.M. Hyperelastic properties of bamboo cellulosic fibre-reinforced silicone rubber biocomposites via compression test. *Int. J. Mol. Sci.* **2022**, *23*, 6338. [[CrossRef](#)] [[PubMed](#)]
12. Feng, Q.K.; Zhang, D.L.; Zha, J.W.; Yin, L.J.; Dang, Z.M. Thermal, electrical, and mechanical properties of addition-type liquid silicone rubber co-filled with Al₂O₃ particles and BN sheets. *J. Appl. Polym. Sci.* **2020**, *137*, 49399. [[CrossRef](#)]
13. Hussain, A.R.J.; Alahyari, A.A.; Eastman, S.A.; Thibaud-Erkey, C.; Johnston, S.; Sobkowicz, M.J. Review of polymers for heat exchanger applications: Factors concerning thermal conductivity. *Appl. Therm. Eng.* **2017**, *113*, 1118–1127. [[CrossRef](#)]
14. Ou, Z.Z.; Gao, F.; Zhao, H.J.; Dang, S.M.; Zhu, L.J. Research on the thermal conductivity and dielectric properties of AlN and BN co-filled addition-cure liquid silicone rubber composites. *RSC Adv.* **2019**, *9*, 28851–28856. [[CrossRef](#)] [[PubMed](#)]
15. Zhang, G.W.; Wang, F.Z.; Dai, J.; Huang, Z.X. Effect of functionalization of graphene nanoplatelets on the mechanical and thermal properties of silicone rubber composites. *Materials* **2016**, *9*, 92. [[CrossRef](#)] [[PubMed](#)]
16. Niu, H.Y.; Ren, Y.J.; Guo, H.C.; Matycha, K.; Orzechowski, K.; Bai, S.L. Recent progress on thermally conductive and electrical insulating rubber composites: Design, processing and applications. *Compos. Commun.* **2020**, *22*, 100430. [[CrossRef](#)]
17. Nguyen, N.; Dinh, V.; Nguyen-Duc, T.; Ta, Q.; Dao, X.; Pham, T.; Nguyen-Duc, T. Effect of potting materials on LED bulb's driver temperature. *Microelectron. Reliab.* **2018**, *86*, 77–81. [[CrossRef](#)]

18. Liquid Silicone Rubbers for Electrical & Electronic Applications. Available online: http://www.shinetsusilicone-global.com/catalog/pdf/LiquidSiliconeRubbers-ele_E.pdf (accessed on 2 May 2022).
19. Grundke, K.; Michel, S.; Knispel, G.; Grundler, A. Wettability of silicone and polyether impression materials: Characterization by surface tension and contact angle measurements. *Colloids Surf. A Physicochem. Eng. Asp.* **2008**, *317*, 598–609. [[CrossRef](#)]
20. Vudayagiri, S.; Junker, M.D.; Skov, A.L. Factors affecting the surface and release properties of thin polydimethylsiloxane films. *Polym. J.* **2013**, *45*, 871–878. [[CrossRef](#)]
21. Chang, H.W.; Wan, Z.M.; Chen, X.; Wan, J.H.; Luo, L.; Zhang, H.N.; Shu, S.M.; Tu, Z.K. Temperature and humidity effect on aging of silicone rubbers as sealing materials for proton exchange membrane fuel cell applications. *Appl. Therm. Eng.* **2016**, *104*, 472–478. [[CrossRef](#)]
22. Yao, Y.; Lu, G.; Boroyevich, D.; Ngo, K.D.T. Survey of High-Temperature polymeric encapsulants for power electronics packaging. *IEEE Trans. Comp. Pack. Man.* **2015**, *5*, 168–181.
23. Chan, S.I.; Hong, W.S.; Kim, K.T.; Yoon, Y.G.; Han, J.H.; Jang, J.S. Accelerated life test of high power white light emitting diodes based on package failure mechanisms. *Microelectron. Reliab.* **2011**, *51*, 1806–1809. [[CrossRef](#)]
24. Pan, B.; Wang, Y.; Jin, J.M.; Wang, L.; Ma, M.D. Mechanical shock ability of different potting materials and packaging processes for electronic components. *Appl. Mech. Mater.* **2012**, *271–272*, 50–54. [[CrossRef](#)]
25. Bloomfield, L.A. Primer system for bonding conventional adhesives and coatings to silicone rubber. *Int. J. Adhes. Adhes.* **2016**, *68*, 239–247. [[CrossRef](#)]
26. Grard, A.; Belec, L.; Perrin, F.X. Effect of surface morphology on the adhesion of silicone elastomers on AA6061 aluminum alloy. *Int. J. Adhes. Adhes.* **2020**, *102*, 102656. [[CrossRef](#)]
27. Roth, J.; Albrecht, V.; Nitschke, M.; Bellmann, C.; Simon, F.; Zschoche, S.; Michel, S.; Luhmann, C.; Grundke, K.; Voit, B. Surface functionalization of silicone rubber for permanent adhesion improvement. *Langmuir* **2008**, *24*, 12603–12611. [[CrossRef](#)] [[PubMed](#)]
28. Abbasi, F.; Mirzadeh, H.; Katbab, A. Modification of polysiloxane polymers for biomedical applications a review. *Polym. Int.* **2001**, *50*, 1279–1287. [[CrossRef](#)]
29. Zhao, M.; Feng, Y.; Li, Y.; Li, G.; Wang, Y.; Han, Y.; Sun, X.; Tan, X. Fabrication of siloxane hybrid material with high adhesion and high refractive index for light emitting diodes (LEDs) encapsulation. *J. Macromol. Sci. A* **2014**, *51*, 653–658. [[CrossRef](#)]
30. Pan, Z.Q.; Huang, B.S.; Zhu, L.Q.; Zeng, K.L. Synthesis of siloxane oligomers containing boron and epoxy groups for promoting the adhesion of addition-curable silicone rubber to PPA and copper plate. *J. Adhes. Sci. Technol.* **2021**, *35*, 626–640. [[CrossRef](#)]
31. Wu, J.K.; Zheng, K.W.; Nie, X.C.; Ge, H.R.; Wang, Q.Y.; Xu, J.T. Promoters for improved adhesion strength between Addition-Cured liquid silicone rubber and Low-Melting-Point thermoplastic polyurethanes. *Materials* **2022**, *15*, 991. [[CrossRef](#)]
32. Pan, K.X.; Zeng, X.R.; Li, H.Q.; Lai, X.J. Synthesis of silane oligomers containing vinyl and epoxy group for improving the adhesion of addition-cure silicone encapsulant. *J. Adhes. Sci. Technol.* **2016**, *30*, 1131–1142. [[CrossRef](#)]
33. Pan, K.X.; Zeng, X.R.; Li, H.Q.; Lai, X.J.; Chen, Z.H.; Liang, G.Q. Synthesis of phenyl silicone resin with epoxy and acrylate group and its adhesion enhancement for addition-cure silicone encapsulant with high refractive index. *J. Adhes. Sci. Technol.* **2016**, *30*, 2699–2709. [[CrossRef](#)]
34. Wang, Y.; Zhang, B.; Zhou, S.T.; Chen, Y.; Liang, M.; Zou, H.W. Preparation of high-performance epoxy-containing silicone rubber via hydrosilylation reaction. *J. Appl. Polym. Sci.* **2019**, *137*, 48397. [[CrossRef](#)]
35. Wang, W.J.; Perng, L.H.; Hsiue, G.H.; Chang, F.C. Characterization and properties of new silicone-containing epoxy resin. *Polymer* **2000**, *41*, 6113–6122. [[CrossRef](#)]
36. Singh, G.P.; Kaur, P.; Kaur, S.; Arora, D.; Singh, P.; Singh, D.P. Density and FTIR studies of multiple transition metal doped Borate Glass. *Mater. Phys. Mech.* **2012**, *14*, 31–36.
37. Clary, J.W.; Rettenmaier, T.J.; Snelling, R.; Bryks, W.; Banwell, J.; Wipke, W.T.; Singaram, B. Hydride as a leaving group in the reaction of pinacolborane with halides under ambient grignard and barbiere conditions. One-Pot synthesis of alkyl, aryl, heteroaryl, vinyl, and allyl pinacolboronic esters. *J. Org. Chem.* **2011**, *76*, 9602–9610. [[CrossRef](#)]
38. Zhai, Q.Q.; Zhao, S.G.; Zhou, C.J.; Li, W.J.; Peng, C. Determination of the Si-H content of hydrogen silicone oil by a combination of the fourier transform near infrared, attenuated total reflectance-fourier transform infrared, and partial least squares regression models. *J. Appl. Polym. Sci.* **2014**, *131*, 40694. [[CrossRef](#)]
39. Hastings, D.L.; Schoenitz, M.; Ryan, K.M.; Dreizin, E.L.; Krumpfer, J.W. Stability and ignition of a siloxane-coated magnesium powder. *Prop. Explos. Pyrotech.* **2020**, *45*, 621–627. [[CrossRef](#)]
40. Gupta, S.; Ramamurthy, P.C.; Madras, G. Covalent Grafting of Polydimethylsiloxane over Surface-Modified Alumina Nanoparticles. *Ind. Eng. Chem. Res.* **2011**, *50*, 6585–6593. [[CrossRef](#)]
41. Yahya, S.N.; Lin, C.K.; Ramli, M.R.; Jaafar, M.; Ahmad, Z. Effect of cross-link density on optoelectronic properties of thermally cured 1,2-epoxy-5-hexene incorporated polysiloxane. *Mater. Des.* **2013**, *47*, 416–423. [[CrossRef](#)]
42. Langer, S.H.; Elbling, I.N.; Finestone, A.B.; Thomas, W.R. The chemistry of new latent curing systems for epoxy resins. *J. Appl. Polym. Sci.* **1961**, *5*, 370–374. [[CrossRef](#)]
43. DOWSIL™ SE 1816 CV Kit. Available online: <https://www.dow.com/documents/en-us/productdatasheet/11/11-32/11-3268-dowsil-se-1816-cv-kit.pdf> (accessed on 15 July 2022).

-
44. Shimpi, T.M.; Moffett, C.; Sampath, W.S.; Barth, K.L. Materials selection investigation for thin film photovoltaic module encapsulation. *Sol. Energy* **2019**, *187*, 226–232. [[CrossRef](#)]
 45. Hacke, P.; Spataru, S.; Terwilliger, K.; Perrin, G.; Glick, S.; Kurtz, S.; Wohlgemuth, J. Accelerated testing and modeling of Potential-induced degradation as a function of temperature and relative humidity. *IEEE J. Photovolt.* **2015**, *5*, 1549–1553. [[CrossRef](#)]